

Original citation:

Hsu, T. I., Calway, A. D. and Wilson, Roland, 1949- (1992) Analysis of structured texture using the multiresolution Fourier transform. University of Warwick. Department of Computer Science. (Department of Computer Science Research Report). (Unpublished) CS-RR-226

Permanent WRAP url:

<http://wrap.warwick.ac.uk/60915>

Copyright and reuse:

The Warwick Research Archive Portal (WRAP) makes this work by researchers of the University of Warwick available open access under the following conditions. Copyright © and all moral rights to the version of the paper presented here belong to the individual author(s) and/or other copyright owners. To the extent reasonable and practicable the material made available in WRAP has been checked for eligibility before being made available.

Copies of full items can be used for personal research or study, educational, or not-for-profit purposes without prior permission or charge. Provided that the authors, title and full bibliographic details are credited, a hyperlink and/or URL is given for the original metadata page and the content is not changed in any way.

A note on versions:

The version presented in WRAP is the published version or, version of record, and may be cited as it appears here. For more information, please contact the WRAP Team at: publications@warwick.ac.uk



<http://wrap.warwick.ac.uk/>

Research Report 226

Analysis of Structured Texture Using the Multiresolution Fourier Transform

Tao-I Hsu, A.D. Calway and R. Wilson

RR226

A multiresolution approach to the analysis of structural texture is presented. The multiresolution Fourier transform (MFT) is utilized as a framework to derive a robust algorithm which estimates textural features over a range of spatial scales based on local frequency domain properties. A pair of centroids of local spectra are extracted to represent the dominant frequencies of underlying spatial regions which are equivariant to rotation and scaling. Based on these centroids, the relationship between two different local spectra is characterized by an affine transformation. Assessment of the estimated affine transform is made by normalized correlation, which also provides local phase shift information. Analysis and synthesis of both artificial and natural images demonstrate the capability of the algorithm.



List of Figures

1	Texture images: brick wall and wall paper pattern	1
2	Outline of algorithm	7
3	Dividing window and Minimum σ_{12}^2 splits local spectrum evenly . . .	8
4	Eight possible transform matrices	10
5	Relationship between <i>from-region</i> , <i>to-region</i> and <i>new-region</i>	11
6	MFT 2-D structure	12
7	Windowed Fourier spectrum	13
8	Original 512×512 FM pattern	i
9	Original 128×128 FM pattern	ii
10	MFT coefficient field at level 5	iii
11	<i>From-block</i> , <i>to-block</i> and eight transformed blocks	iv
12	Plot of variance vs. rotation degree (one feature case)	v
13	Plot of variance vs. rotation degree (two features case)	vi
14	Algorithm failed when the MFT block of size 64×64	vii
15	Smaller MFT block size (32×32) solves the mistaken selection	viii
16	FM pattern synthesis at MFT level 6	ix
17	FM pattern synthesis at MFT level 5	x
18	FM pattern synthesis at MFT level 4	xi
19	Entire FM pattern synthesis at MFT level 5	xii
20	Entire FM pattern synthesis at MFT level 4	xiii
21	Original reptile pattern	xiv
22	Reptile pattern synthesis at MFT level 5	xv
23	Reptile pattern synthesis at MFT level 3,4,5 and 6	xvi
24	The significance of different functions	xvii

1 Introduction

Texture is one of the important characteristics which exists in natural image. There are several different definitions of texture. Hawkins gave a definition of texture as follows [9]:

"the notation of texture appears to be depended upon three ingredients: a. some local "order" is repeated over a region which is large in comparison to the order's size b. the order consists non-random arrangement of elementary parts c.the parts are roughly uniform entities having approximately the same dimensions everywhere within the textured region".

A large class of textures could be covered by such a definition, for example, a brick wall or a wall paper pattern as shown in figure 1.

In image texture analysis, the objective is to discover the useful features that describe the coarseness, directionality and regularity of image texture. There are two main approaches to texture image analysis. The statistical approach [8] attempts a global characterization of texture. Statistical properties of the image gray level are measured as texture descriptors. This approach deals with properties of individual image pixels instead of subregions. The structural approach [8] views textures as an arrangement of a set of textural elements according to certain placement rules. Their major purpose is to give a compact structural description of texture by a minimum number of parameters. Statistical models may be successfully used in discriminating sets of textures. However, since texture is often piecewise uniform with respect to some structural properties, the structural approach is equally powerful in modeling texture in many cases. In structural textures, the basic elements themselves, in general, may also be made up of a set of texture elements, ie., they may be microtextured.

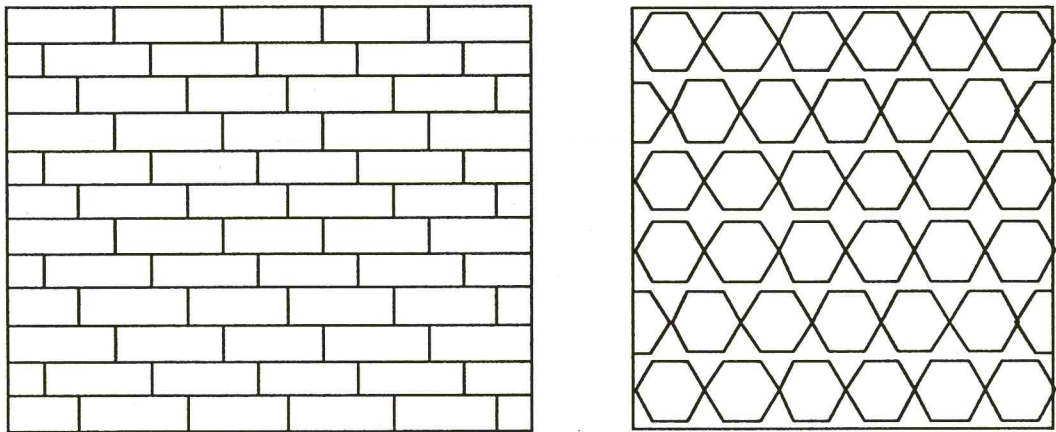


Figure 1: Texture images: brick wall and wall paper pattern

This leads us to model texture hierarchically in a way which requires no *a priori* knowledge of the scale of texture elements. Haralick [8] used the co-occurrence matrix to measure the features of texture elements based on the length of similar pixel grey level values within a given neighbourhood. His method is limited to describing the texture element's local variation in orientation and requires the size of neighbourhood. Bajcsy [3] used statistical measurement derived from the Fourier power spectrum of the image to detect the global periodicity by identifying high-energy, narrowed peaks in the spectrum, although the approach is not invariant to changes in either orientation or scale.

This report is motivated by the need for a texture representation which is hierarchical and invariant to elementary geometric transformation, such as rotation, scaling and translation, with the capability of capturing both local and global texture information simultaneously. Towards this end, a new model for texture feature representation based on the multiresolution Fourier transform (MFT) [5] is described. The MFT is a linear transform providing local frequency estimation over multiple spatial resolutions and is thus ideally suited to the analysis of local frequency properties of textural elements at different scales. Local spectra within the MFT corresponding to image regions at different scales are represented by a pair of centroid vectors which are estimated using a *minimum variance* criterion and are equivariant to rotation and scaling. Using these vectors, the affine transform between two different regions is then obtained and an assessment of the transform selection is done using normalized correlation. From the correlation, the phase information about the position shift between two local spectra is also obtained.

A literature review is presented at section 1. Existing structural texture feature representation schemes are reviewed and a comparison is made between the existing models in terms of various textural measures such as locality, rotation, scale and orientation in the texture features. The new approach to texture feature representation is described in section 3, and its implementation using the MFT is described in section 4. The MFT's capability and elementary properties are discussed. In section 5, the effectiveness of the approach is demonstrated by the analysis and synthesis of natural and synthetic images. The report concludes with a discussion of future investigations into the properties of the algorithm.

2 Survey of structural texture analysis schemes

The schemes reviewed in this section are divided into two broad categories: spatial-domain methods and frequency-domain methods. Processing techniques in the first category are based on direct manipulation of the pixels in an image. A typical example is the co-occurrence matrix method [8]. The frequency domain, on the other hand, refers to the transformed field of an image, and approaches in this category are based

on the processing of the frequency energy in the spectrum of image. An example of this approach is the power spectrum method [3].

2.1 Spatial domain approaches

Co-occurrence matrix

The spatial gray level dependence method is based on the estimation of the second-order joint conditional probability density function, $f(i, j|d, \theta)$. Each $f(i, j|d, \theta)$ is the probability of going from gray level i to gray level j , given the intersample spacing distance d , and the direction is given by the angle θ . The estimated values, $x_\theta(i, j|d)$, can be written in matrix form, the so-called co-occurrence matrix.

From a co-occurrence matrix a number of texture features can be defined, such as

1. Energy:

$$E(x_\theta(d)) = \sum_i \sum_j [x_\theta(i, j|d)]^2 \quad (1)$$

2. Entropy:

$$H(x_\theta(d)) = - \sum_i \sum_j [x_\theta(i, j|d)] \log x_\theta(i, j|d) \quad (2)$$

3. Correlation:

$$R(x_\theta(d)) = \frac{\sum_i \sum_j (i - \mu_i)(j - \mu_j) x_\theta(i, j|d)}{\sigma_i \sigma_j} \quad (3)$$

4. Local Homogeneity:

$$L(x_\theta(d)) = \sum_i \sum_j \frac{1}{1 + (i - j)^2} x_\theta(i, j|d) \quad (4)$$

5. Inertia:

$$I(x_\theta(d)) = \sum_i \sum_j (i - j)^2 x_\theta(i, j|d) \quad (5)$$

Various versions of co-occurrence matrixes have been developed and its capability has been demonstrated [6]. As we can see from the above textural features description, the intersample spacing distance d plays a dominant role in determining the processing power of co-occurrence methods. The textural structures which can be described within a neighborhood are naturally limited to those which are observable within the size of the neighborhood. Thus a feature, based on measurements within a neighborhood, fixed in size, has a poor discrimination power when applied to a texture not observable within the neighborhood because of the wrong scale. But in general the size information is not available. There are other problems associated with co-occurrence matrix method.

1. A co-occurrence matrix must be computed for each value of θ and d . This requires a fair amount of computation.
2. Co-occurrence matrices are inappropriate to describe oriented texture. This is because the co-occurrence matrix is defined only for globally discrete value of θ , and is hence incapable of estimation local variations in orientation.
3. In order to reduce the dimensionality of the feature vector, detailed first stage classification experiments are needed to determine the best reduced sets of features to use for successful classification.
4. The feature representation is not rotation invariant (except to multiples of 45°) or scale change in the texture.
5. The classifier lacks any claim to optimality.

2.2 Frequency domain approach

Power spectrum method

Compared with spatial domain approaches, the frequency domain approach is preferable, for two reasons. First, an effective textural feature descriptor should be able to describe the spatial arrangement of the texture element as well as to express the size and shape of the texture elements simultaneously. From the elementary properties of Fourier transform, for any real periodic function its Fourier spectrum is symmetrical with respect to origin, and the Fourier spectrum is translation invariant. Therefore, the periodical or partially periodical function could be represented more concisely in terms of the Fourier spectrum of an image. Secondly, if there is noise within the textural image, the noise process will alter image representation dramatically in spatial domain, but uniformly in frequency domain. Hence, the frequency measure should be less sensitive to the noise than that in the spatial domain. Bajcsy [3] used statistical measures derived from the Fourier power spectrum of the image. One of the most significant pieces of information about an image revealed by means of Fourier power spectrum methods is periodicity.

Rosenfeld, et.al., [10] used ring-shaped and wedge-shaped samples of the discrete Fourier power spectrum to obtain the information of the size texture element and orientation of the texture image. Let $p(\cdot, \cdot)$ be the power spectrum obtained from a local region of an image.

1. Periodicity: this feature is related to energy in major peak.

$$periodicity = \frac{p(u_{peak}, v_{peak})}{\sum_{u,v \neq 0} p(u, v)} \quad (6)$$

2. Size of texture element: this feature is based on ring-shaped samples which are of the form

$$\Phi_{r_1, r_2} = \sum_{r_1^2 \leq u^2 + v^2 \leq r_2^2} p(u, v) \quad (7)$$

3. Orientation: this feature is based on wedge-shaped samples which are of the form

$$\Phi_{\theta_1, \theta_2} = \sum_{\theta_1 \leq \arctan(\frac{v}{u}) \leq \theta_2} p(u, v) \quad (8)$$

There are few difficulties associated with these statistical measures:

1. They are not invariant to change of texture element in either orientation or scale.
2. The ring and wedge shaped functions used to compute the texture feature were based on a windowed Fourier transform. Spatial locality is introduced by windowing the data prior to the integration of the energy of the transformed windowed data. However, this involves a loss in spatial frequency resolution as the spectrum of the image is now convolved with that of the spatial window.

2.3 Summary

The requirements of a suitable textural image descriptor can be summarized as following.

1. Coarseness in textural features is always scale dependent. This scale characteristic should be resolved in the feature descriptor to allow the image to be analysed at different scales.
2. The information of feature should be retained in both the spatial domain and frequency domain to achieve optimality.
3. The translation and orientation of the texture elements should be represented in the descriptor with properties of translation and orientation invariance.
4. The descriptor should be able to describe the global and local information corresponding to the spatial distribution and size of the texture element respectively.
5. The computational requirements should not be excessive so as inhibit implementation of the descriptor.
6. The model should be capable of dealing with noise.
7. The most important desired property relating to the descriptor is that the descriptor should be a signal based model without *a priori* knowledge of the input.

3 Affine transformation estimation

The new approach to the analysis of texture elements is presented in this section. The scheme is based on the following assumptions:

1. The underlying texture element can be characterized in the frequency domain by local concentrations of energy about one or two frequencies.
2. Elements of the same texture are related via an affine transformation, ie. they are rotated, scaled and translated version of each other.

The aim of the analysis is first to derive a representation of such elements and subsequently to estimate the associated affine relationship amongst the elements. There are two phases in this analysis: phase 1 is to generate a pair of centroid vectors which are equivariant to rotation and scaling, while phase 2 is to estimate the affine transformation based on the estimated centroid vectors. Figure 2 illustrates the main components of the algorithm and these are described in detail below. The notation used in this section is as follows: consider a 2-D discrete image $x(\vec{\xi}_k)$ which is tessellated into a number of small lattice squares and let $\hat{x}(\vec{\xi}_i, \vec{\omega}_j, \sigma)$ be a local discrete Fourier spectral estimate for a region centered at spatial position $\vec{\xi}_i$ and at scale σ , where $\vec{\xi}_i = (\xi_{i1}, \xi_{i2})$ is the coordinate in 2-D space.

3.1 Affine transform

A linear transformation followed by a translation is an affine transformation T , ie.

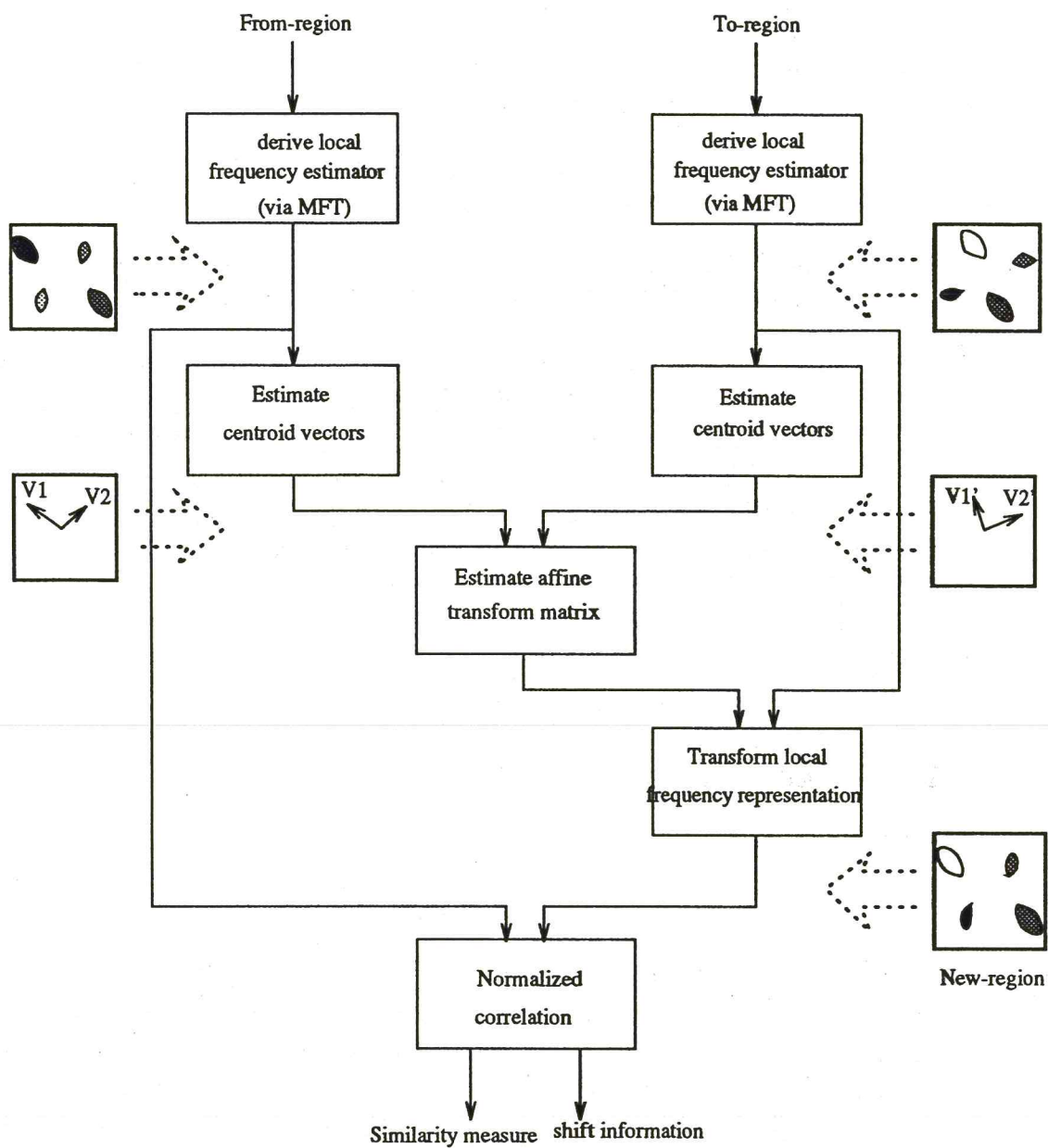
$$T\vec{\xi} = A\vec{\xi} + \gamma \quad (9)$$

where A is a matrix, and γ is translation term. Thus, the affine transform is actually a combination of scaling, rotation and translation. Based on the affine transform, the spatial distribution of texture elements could be characterized. In order to estimate the affine transformation between two different regions, R_{from} and R_{to} , the two pairs of vectors which could represent R_{from} and R_{to} correspondingly ought to be located first.

3.2 Estimation of centroid vectors

3.2.1 Centroid vectors calculation

In the frequency domain, there exists the symmetrical property. Hence the computation size requirement to estimate the centroid vectors in frequency domain is only half dimension of $\hat{x}(\vec{\xi}_i, \vec{\omega}_j, \sigma)$. Moreover, the centroid vectors should be located far enough apart to carry out the affine transformation effectively. This introduces a



Different fill-mode within blobs stands for phase difference of local spectrum

Figure 2: Outline of algorithm

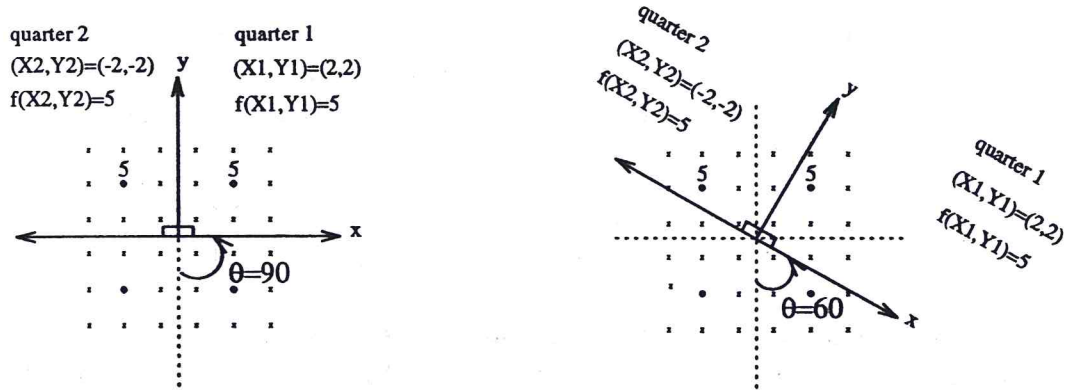


Figure 3: Dividing window and Minimum σ_{i2}^2 splits local spectrum evenly

dividing window '⊥' to divide $\hat{x}(\vec{\xi}_i, \vec{\omega}_j, \sigma)$ into three subregions, two quarters and one half. Let $\vec{\mu}_{ik}(\theta)$ and $\sigma_{ik}^2(\theta)$ be the centroid and variance of quarter k , $k = 1, 2$, at each angle θ of the dividing window '⊥' for spatial position $\vec{\xi}_i$.

$$\begin{aligned}\vec{\mu}_{ik}(\theta) &= \frac{1}{E_{ik}(\theta)} \sum_{\vec{\omega}_j \in \Lambda_k(\theta)} \vec{\omega}_j |\hat{x}(\vec{\xi}_i, \vec{\omega}_j, \sigma)| \\ \sigma_{ik}^2(\theta) &= \frac{1}{E_{ik}(\theta)} \sum_{\vec{\omega}_j \in \Lambda_k(\theta)} \vec{\omega}_j \cdot \vec{\omega}_j |\hat{x}(\vec{\xi}_i, \vec{\omega}_j, \sigma)|\end{aligned}\quad (10)$$

where

$$E_{ik}(\theta) = \sum_{\vec{\omega}_j \in \Lambda_k(\theta)} |\hat{x}(\vec{\xi}_i, \vec{\omega}_j, \sigma)|$$

and $\Lambda_k(\theta)$ is the set of coefficients in quarter k and ' \cdot ' is inner product. Rotating the dividing window '⊥' from 0° to 180° and selecting the best angle avoids the local concentrating energy lying along the dividing window '⊥'.

3.2.2 Minimum variance criterion

The sum of the variance of the two quarter regions, with respect to the estimated centroids is used as a criterion selection. This is defined as equation (11). By determining the angle at which this variance is minimum, the dividing window '⊥' then evenly splits the local spectra into two separate regions, see figure 3.

$$\sigma_{i12}^2(\theta) = \sigma_{i1}^2(\theta) + \sigma_{i2}^2(\theta) \quad (11)$$

The centroids of the corresponding quarters then defines the required equivariant vectors.

3.3 Estimation of affine matrix

The algorithm proceeds with obtaining the transform matrix to estimate the affine transformation between two regions, R_1 and R_2 . Based on the estimated centroid pair $(\vec{\mu}_{i1}, \vec{\mu}_{i2})$ and $(\vec{\mu}'_{i1}, \vec{\mu}'_{i2})$, a linear transformation matrix, A , can be found by calculating the linear equation (12).

$$\begin{bmatrix} \vec{\mu}'_{i1} \\ \vec{\mu}'_{i2} \end{bmatrix} = A \begin{bmatrix} \vec{\mu}_{i1} \\ \vec{\mu}_{i2} \end{bmatrix} = \begin{bmatrix} a_{11} & a_{12} \\ a_{21} & a_{22} \end{bmatrix} \begin{bmatrix} \vec{\mu}_{i1} \\ \vec{\mu}_{i2} \end{bmatrix} \quad (12)$$

There are eight different possible matrixes, A_i ; $i = 1, \dots, 8$ see figure (4). A_1 is formed by calculating from centroid pair $(\vec{\mu}_{i1}, \vec{\mu}_{i2})$ to $(\vec{\mu}'_{i1}, \vec{\mu}'_{i2})$, as equation (12). A_2 is obtained from A_1 by swapping centroid pair from $(\vec{\mu}'_{i1}, \vec{\mu}'_{i2})$ to $(\vec{\mu}'_{i2}, \vec{\mu}'_{i1})$. A_3 is formed by means of replacing $\vec{\mu}'_{i2}$ by $-\vec{\mu}'_{i2}$. A_4 is to swap centroid pair from that of A_3 same way as A_2 swapped from A_1 . A_j , $j = 5, \dots, 8$ are obtained from A_i , $i = 1, \dots, 4$ respectively by negating $(\vec{\mu}'_{i1}, \vec{\mu}'_{i2})$.

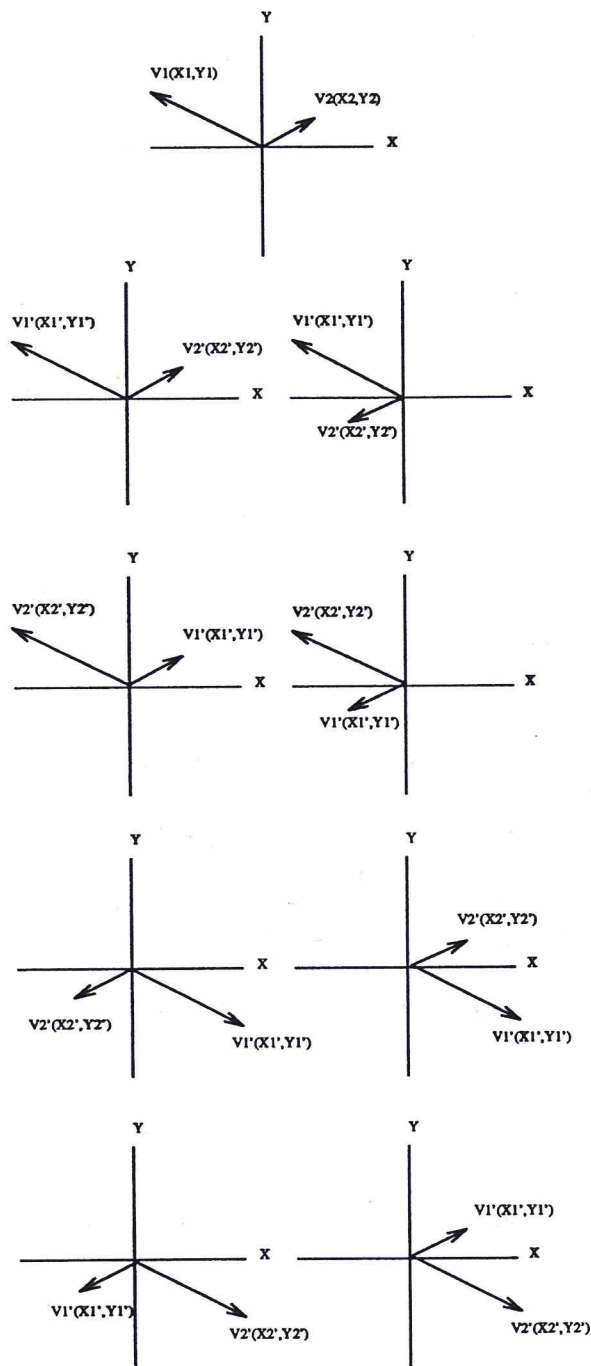
3.4 Region transformation and correlation

Eight transformed regions, the *new-regions*, are created by using the eight transform matrixes obtained from section 3.3, A_i ; $i = 1, \dots, 8$, to perform coordinate transform and bi-linear interpolate pixel value from the the region where the *from-region* is transformed to, the *to-region*. The relationship among *from-region to-region* and *new-region* is shown in figure 5. The maximum correlation coefficient between the *from-region* and 8 *new-regions* decides the best affine transform matrix and provides the phase shift information. The decision is made according to the normalized correlation between the *new-region* and the region where the *new-region* is transformed from, the *from-region*. If the transform matrix is the correct selection, the *new-region* will be similar to the *from-region*.

The normalized correlation [7] is performed directly in frequency domain by applying the energy theorem [11]

$$\rho_i(k, l) = \frac{F^{-1}[\hat{x}(\vec{\xi}_k, \vec{\omega}_j, \sigma) \hat{x}_i^*(\vec{\xi}_l, \vec{\omega}_j, \sigma)]}{\sum_j |\hat{x}(\vec{\xi}_k, \vec{\omega}_j, \sigma)|^2 |\hat{x}_i(\vec{\xi}_l, \vec{\omega}_j, \sigma)|^2} \quad (13)$$

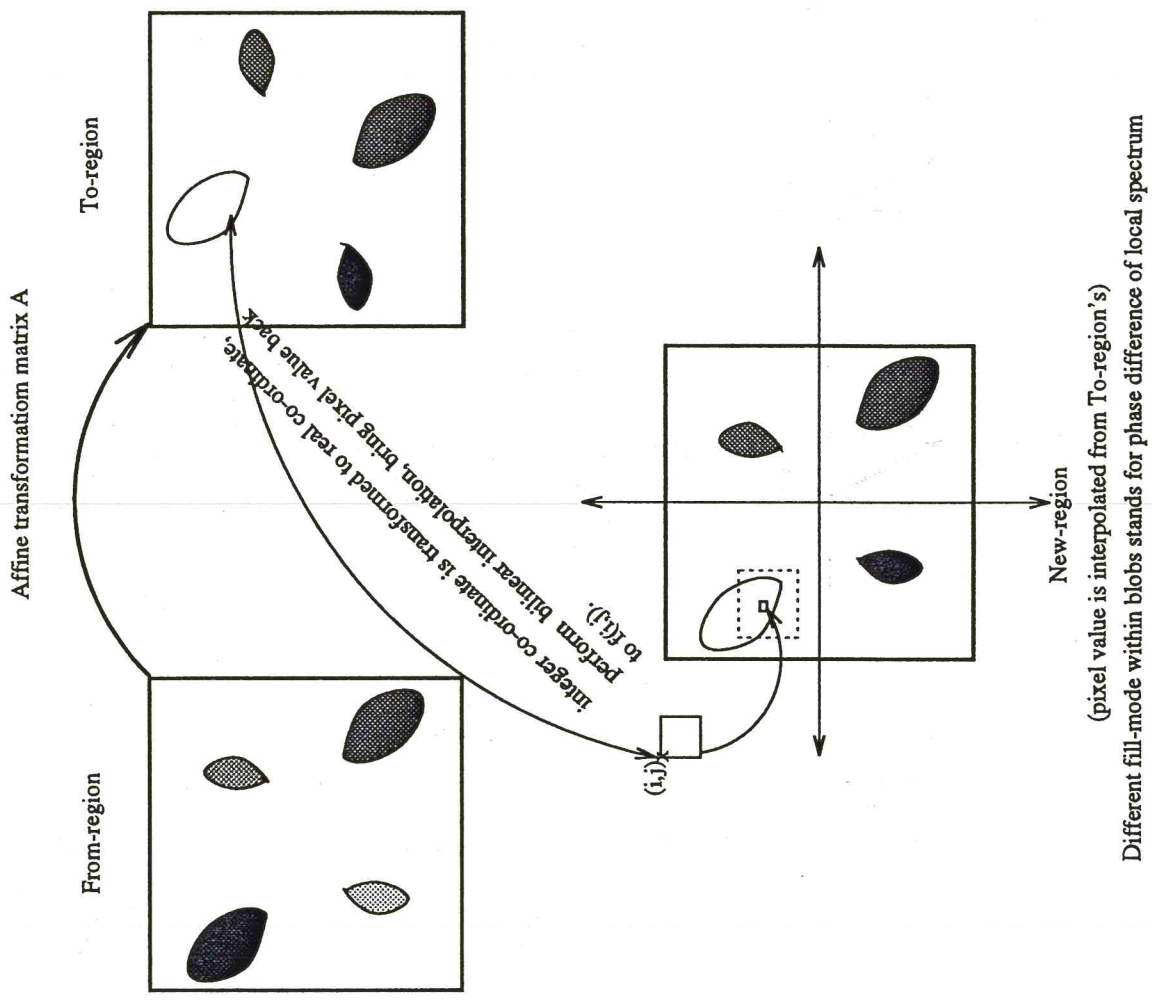
where F^{-1} denotes the 2-D inverse Fourier transform, $\hat{x}_i(\vec{\xi}_l, \vec{\omega}_j, \sigma)$ is the local spectra of *new-region*, $i = 1, \dots, 8$ and '*' is complex conjugate. The transformation matrix is selected corresponding to maximum $\rho_i(k, l)$.



centroid pair to form transform matrix

from-region	
to-region 1	to-region 3
to-region 2	to-region 4
to-region 5	to-region 7
to-region 6	to-region 8

Figure 4: Eight possible transform matrices



(pixel value is interpolated from *to-region*'s)
 Different fill-mode within blobs stands for phase difference of local spectrum

Figure 5: Relationship between *from-region*, *to-region* and *new-region*

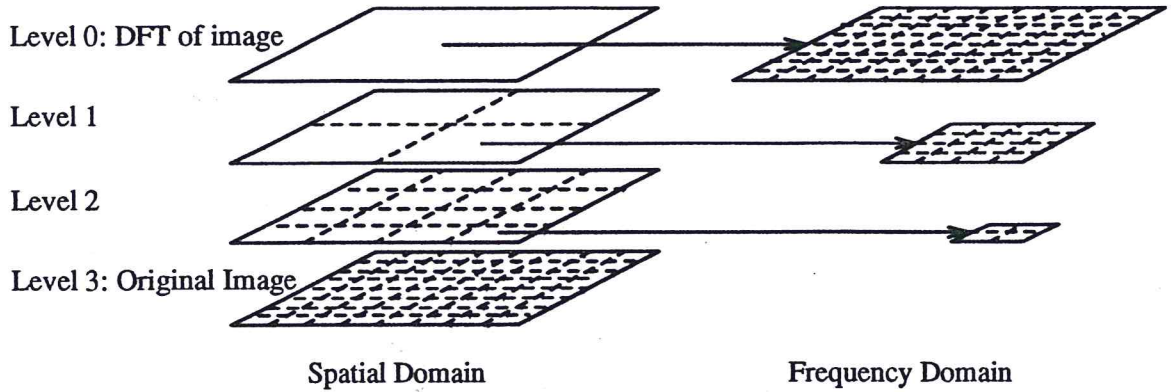


Figure 6: MFT 2-D structure

4 Implementation

4.1 Multiresolution Fourier Transform

Central to the above analysis is the availability of local frequency estimates over multiple scales. These can be obtained from the MFT of the texture image. The MFT is a generalized form of wavelet transform [1] and [2]. The MFT is to have scale σ as part of a signal representation in phase-space (ξ, ω) so that MFT is able to perform local Fourier analysis at various scales. The general structure of the MFT is shown in figure 6. This section briefly introduces the properties of MFT.

4.1.1 Continuous case

In $1 - D$ continuous case, for a given signal $\hat{x}(\xi)$, the definition of MFT is

$$\hat{x}(\xi, \omega, \sigma) = \sigma^{1/2} \int_{-\infty}^{\infty} d\chi x(\chi) w(\sigma(\chi - \xi)) \exp[-j\omega\chi] \quad (14)$$

where ξ is the spatial co-ordinate, ω is frequency co-ordinate and $w(\xi)$ is an appropriate windowing function. Thus $\hat{x}(\xi, \omega, \sigma)$ is a windowed Fourier spectrum of a local region in the signal domain centered at spatial position ξ at scale σ with windowing function $w(\xi)$, see figure 7. The extension to m -D continuous MFT is straight forward. Let $\vec{\xi} = (\xi_1, \dots, \xi_m)^T$, then

$$\hat{x}(\vec{\xi}, \vec{\omega}, \sigma) = \sigma^{m/2} \int_{-\infty}^{\infty} d\vec{\chi} x(\vec{\chi}) w(\sigma(\vec{\chi} - \vec{\xi})) \exp[-j\vec{\omega} \cdot \vec{\chi}] \quad (15)$$

where $\vec{\omega}$ is the Fourier co-ordinate.

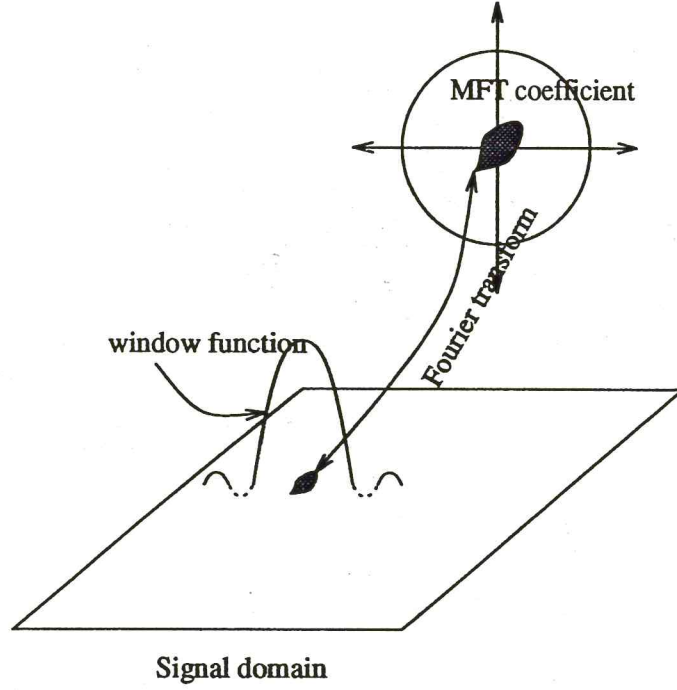


Figure 7: Windowed Fourier spectrum

4.1.2 Discrete case

The 1-D MFT coefficient at scale $\sigma(n)$, position $\xi_i(n)$ and frequency $\omega_j(n)$ can be written as

$$\hat{x}(\xi_i(n), \omega_j(n), \sigma(n)) = \sum_k w_n(\xi_k - \xi_i(n)) x(\xi_k) \exp[-j\xi_k \omega_j(n)] \quad (16)$$

where $w_n(\xi_k)$ is the scale n window sequence, ξ_k is the k th sample point for the original sequence and the sample points at scale n are $\xi_k(n)$ and $\omega_l(n)$ for the original and Fourier co-ordinates respectively. The window function $w(\xi)$ in MFT is a bandlimited Finite Prolate Spheroidal Sequence (FPSS). The FPSS is used as a windowing function with maximal energy concentration in both spatial and frequency domain. The bandlimited form FPSS \mathbf{u} is defined as solution of eigenvalue problem generated in accordance with satisfactoriness of window unambiguity constraint in both spatial and frequency domain. The eigenvalue equation for the FPSS is

$$\mathbf{B}(\Omega)\mathbf{I}(\Xi)\mathbf{B}(\Omega)\mathbf{u} = \lambda\mathbf{u} \quad (17)$$

where $\mathbf{I}(\Xi)$ is the index-limiting operator,

$$I_{ij}(\Xi) = \begin{cases} \delta_{ij} & |\xi_i| < \Xi/2 \\ 0 & \text{else} \end{cases} \quad (18)$$

and $B(\Omega)$ is the bandlimiting operator,

$$B(\Omega) = F^* I(\Omega) F \quad (19)$$

In order to achieve the better localization in spatial domain and reduce the ambiguity, a relaxed version of MFT is used. This is accomplished by oversampling in the spatial domain by factor of 2^k , leading to increased bandwidth in frequency domain by factor of 2^k .

$$\mathbf{w}_n = B(2^k \Omega(n)) I(\Xi_0(n)) \mathbf{u}_n \quad (20)$$

Extension of the 1-D case in (16) to the 2-D case can be achieved using a cartesian separable implementation. Let $N = 2^M$, then $\Xi(n) = 2^{n+1-M}$ and $\Omega(n) = 2^{M-k-n}$. There are $M \times M$ blocks each is size of $N_\Omega(n) \times N_\Omega(n) = 2^n \times 2^n$. As illustration, for example, for a $128 \times 128 = 2^7 \times 2^7$ image, $M = 7$, the MFT of this image at level $n = 5$ is composed of $2^7/2^{5-1} \times 2^7/2^{5-1}$ blocks with each block of size $2^{n=5} \times 2^{n=5}$, the sampling interval in both domain are

$$\Xi(n) = 2^{n+1-M} = 2^{5+1-7} = 0.5 \quad (21)$$

$$\Omega(n) = 2^{M-k-n} = 2^{7-5-2} = 1 \quad (22)$$

5 Experiments

5.1 Centroid Estimation

To test the algorithm, experiments are performed on the FM pattern in figure 8. This FM pattern is generated from both *radial function* and *angular function*. It consists the characteristics of scaling, rotation and translation encountered in general image analysis. Figure 9 is a 128×128 image taken out from the original 512×512 FM pattern and its associated MFT coefficients are shown as figure 10. Figure 11 shows *from-block*, *to-block* and eight possible *new-block* where pixel value interpolated from *to-block*. In the *from-block* and *to-block*, the dividing window '⊥' is overlaid. From the overlaid pattern, the minimum variance criterion does make the dividing window '⊥' split the local spectrum evenly. The *from-block* and *to-block* are two blocks arbitrary chosen from figure 10. In this case, the block 3 is the most similar to *from-block* and it is the rotated version of the *to-block*. The normalized correlation coefficient is 0.9556.

There is an important issue regarding to the number of significant features contained in single MFT block. If there is only one blob, this could be detected by examining the ratio of the variance. Let σ_{12}^2 be the sum of variance of two quarters in division window '⊥' with respect to the estimated centroid pair within these two

quarters respectively and σ_{half}^2 stands for the variance with respect to the centroid within the half block. Then the ratio

$$\frac{\sigma_{12}}{\sigma_{half}} \simeq 1. \quad (23)$$

provided that there is only one significant feature in the block. If there are two features in one block, then the ratio

$$\frac{\sigma_{12}}{\sigma_{half}} \ll 1. \quad (24)$$

In the case of only one feature present, the curve of the σ^2 is shown in figure 12. While in the case of two features, the curve has two extremes, see figure 13. If there are more than two features existing in one block, the algorithm will not be as reliable as the case of less and equal to two features. Further investigation is needed to study this.

In the case of small spatial blocks then it turns out the algorithm will select the wrong transform matrix due to low correlation. Figure 14 shows this situation for MFT level 6 where transformed block 6 is chosen with correlation only 0.194. But this difficulty can be solved by applying different level of MFT to increase the resolution in frequency domain. Figure 15 shows the effectiveness of MFT. In this case we used the MFT level 5 and chosed the same portion of the MFT coefficient field as in figure 14. The block 1 is selected as best affine transform matrix and correlation result is 0.703127. Also note that, the size of the transformed local spectrum in block 1 is scaled down from *to-block* by affine transform.

5.2 Texture synthesis

5.2.1 Procedure analysis

In this section, we outline the procedure of synthesizing (or reconstructing) all other blocks from the *from-block* to give a new synthesized image. After performing normalized correlation in the multiresolution affine transform, the image synthesis is accomplished by following stages.

1. *Phase shift correction*: the phase shift information between the *from-block* and the best *new-block* is provided by the correlation calculation. To correct the position of the *new-block*,

$$\hat{x}'_{newblock}(\vec{\xi}_i, \vec{\omega}_j, \sigma) = \hat{x}_{newblock}(\vec{\xi}_i, \vec{\omega}_j, \sigma) \exp[-j2\pi(\vec{\omega}_j \cdot \vec{d})/N] \quad (25)$$

where \vec{d} is the position of correlation peak and N is block size.

2. *Energy normalization*: energy normalization is used to keep the energy of the synthesized block being the same as that of original block, the *to-block* where the synthesized block is transformed to.
3. *Cosine windowing*: the output of the inverse Fourier transform is twice the size of the original image's due to the MFT *oversampling*. Therefore, we could either take the middle part of the block or perform the cosine windowing function over the inverse Fourier transform output followed by adding them up to give a synthesized image without blocking artefacts.

$$x(\vec{\xi}) = \sum_{\text{newblock}} x_{\text{newblock}}(\vec{\xi}) \cos^2(2\pi\vec{\xi}/N). \quad (26)$$

where

$$x_{\text{newblock}}(\vec{\xi}) = F^{-1}[\hat{x}'_{\text{newblock}}(\vec{\xi}_i, \vec{\omega}_j, \sigma)] \quad (27)$$

5.2.2 Synthesis of FM pattern

This synthesized FM patterns are shown at figures 16, 17 and 18. Figures 16,17 and 18 are results of the algorithm performed over FM pattern size of 128×128 with MFT block size of 64×64 , 32×32 and 16×16 respectively. The blurred portion of these images is caused by the cosine smoothing function over each IFFT of the MFT block. The entire FM pattern synthesized at MFT level 4 and 5 are shown at figures 20 and 19.

5.2.3 Synthesis of natural image

The reptile pattern, figure 21, from the Brodatz's well known album [4] has also been reconstructed at different MFT levels. Figure 22 shows the synthesized reptile image entirely at MFT level 5. In order to compare the effect of differen MFT level, the synthesized reptile images from level 3, 4, 5, and 6 are grouped together, see figure 23 where a. is level 3, b. is level 4, c. is level 5 and d. is level 6. The significance of the energy normalization, coordinate transform and phase position shift are shown at figure 24. This figure shows different stages of the image synthesized procedure at MFT level 3. Each of them affects the synthesized result. In figure 24, a. is synthesized reptile image with energy normalization, affine transform and phase shift correction, b. is the synthesized reptile image produced same procedure as in a. except without enegy normalization, c. is generated without both energy normalization and coordinate transform. The synthesized image still has structure of reptile skin but is more randomized due to lack of the suitable affine transformation. Figure 24 d. is generated from portion of an image without phase shift, coordinate transform and energy normalization. Therefore, the synthesized result is just a repeated copy of the same local portion of the image.

6 Conclusions and Further work

This work has reviewed the literatures on texture analysis. The limitations in scaling, rotation and translation of these methods have been discussed. A new algorithm has been derived to overcome these limitations. This algorithm makes use of the Multiresolution Fourier Transform, or MFT, as a tool to estimate the affine transformation among the MFT coefficient field. The algorithm has successfully characterized the texture element and their spatial distribution simultaneously directly in the frequency domain. The analysis and synthesis of both artificial and natural texture images have shown the potential of the new algorithm.

Incorporation of detection on more than two features presenting in a MFT block into this new algorithm will need to be studied more. A further stage of development would be to combine information from various level and neighbouring blocks. The inclusion of the information in spatial domain is another research direction.

References

- [1] R. Wilson A. Calway, E.R.S. Pearson. A Generalized Wavelet Transform for Fourier Analysis: The Multiresolution Fourier Transform and Its Application to Image and Audio Signal Analysis. *IEEE Trans. I.T.*, 38(2), March 1992.
- [2] R. Wilson A. Calway, E.R.S. Pearson and A. Davies. An Introduction of Multiresolution Fourier Transform and it's applications. Research Report RR204, Department of Computer Science, University of Warwick, UK, January 1992.
- [3] R. Bajcsy. Computer description of textured surfaces. In *Proc. of 3rd Int. Joint Conf. Art. Int.*, pages 572-579, August 1973.
- [4] P. Brodatz. *A Photographic Album for Artists and Designers*. Dover Publishing Company, 1966.
- [5] A. D. Calway. *The Multiresolution Fourier Transform: A general Purpose Tool for Image Analysis*. PhD thesis, Department of Computer Science, The University of Warwick, UK, September 1989.
- [6] R. W. Connors and C. A. Harlow. A Theoretical Comparison of Texture Algorithms. *IEEE Trans. P.A.M.I.*, 2(3):204-222, May 1980.
- [7] R. C. Gonzalez and P. Wintz. *Digital Image Processing (2nd. Ed)*. Addison-Wesley, New York, 1987.
- [8] R. Haralick. Statistical and structural approaches to texture. *IEEE*, 67(5):610-621, 1979.
- [9] J.K. Hawkins. Textural properties for pattern recognition. In B.S. Lipkin and A. Rosenfeld, editors, *Picture Processing and Psycophysics*. New York Academic Press, 1970.
- [10] C.R. Dyer J.S. Weszka and A. Rosenfeld. A Comparative Study of Texture Measures for Terrain Classification. *IEEE Trans. S.M.C*, 6(4):269-285, April 1976.
- [11] A. Papoulis. *Signal Analysis*. McGraw-Hill, 1984.

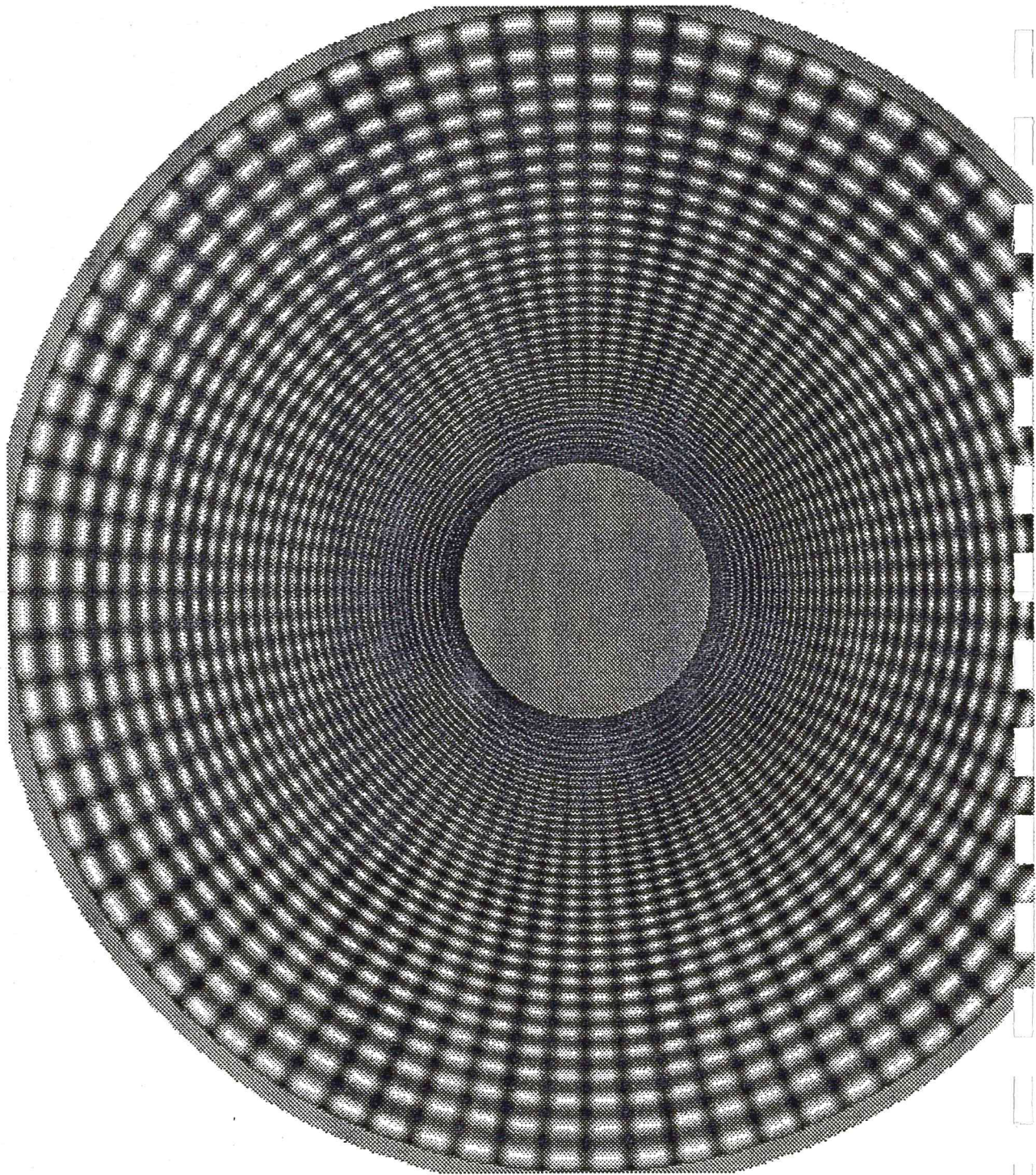


Figure 8: Original 512×512 FM pattern

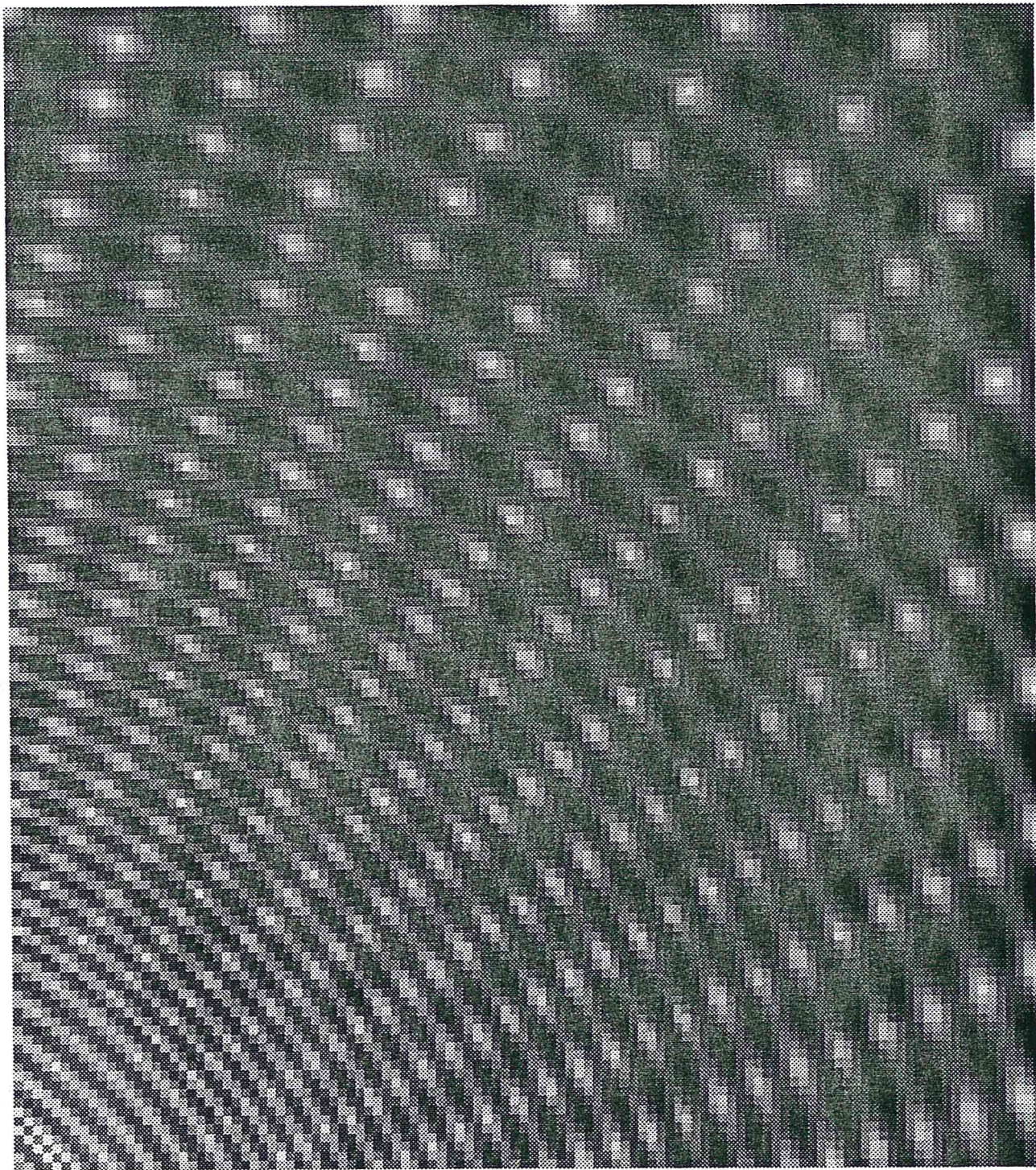


Figure 9: Original 128×128 FM pattern

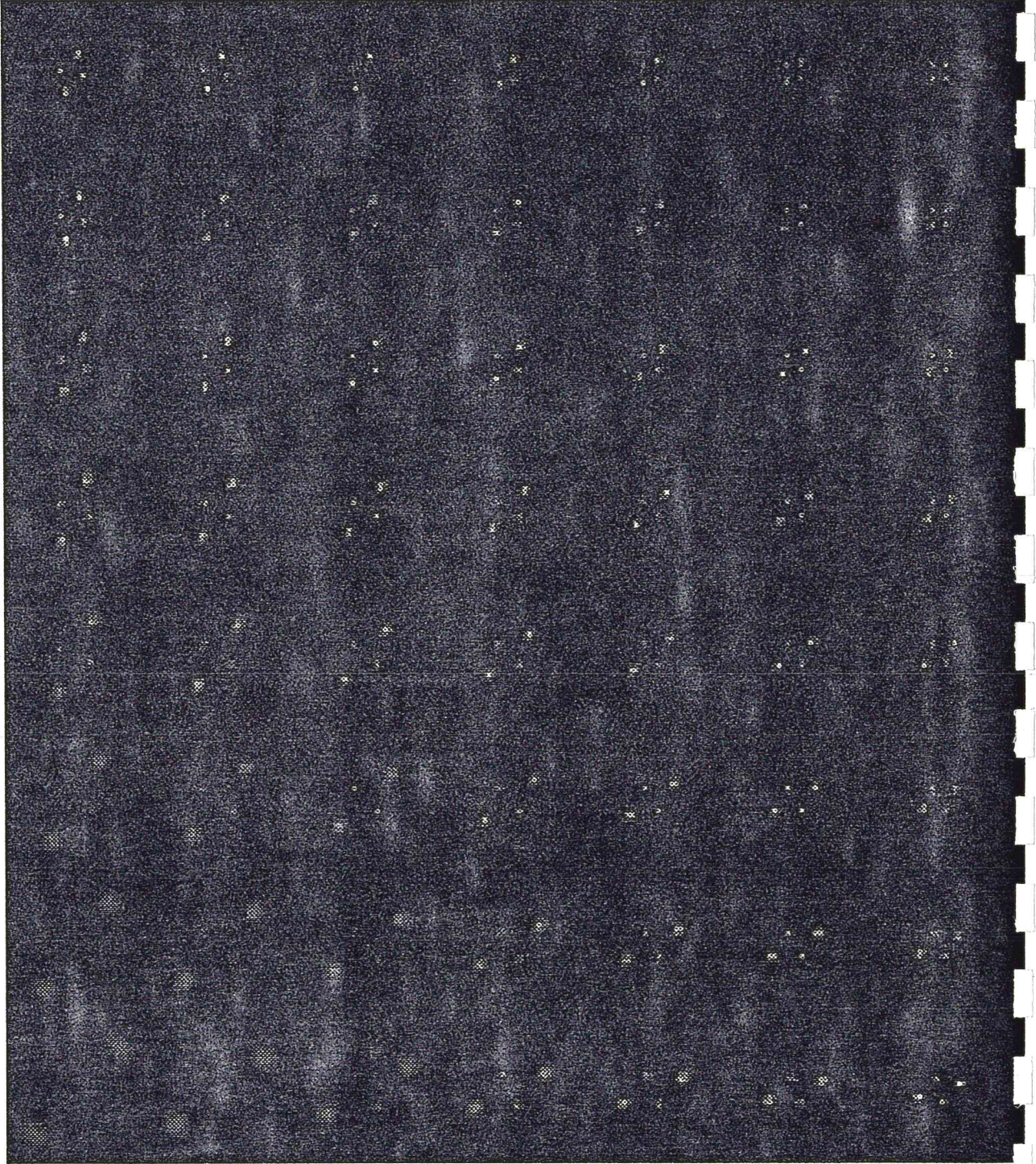


Figure 10: MFT coefficient field at level 5

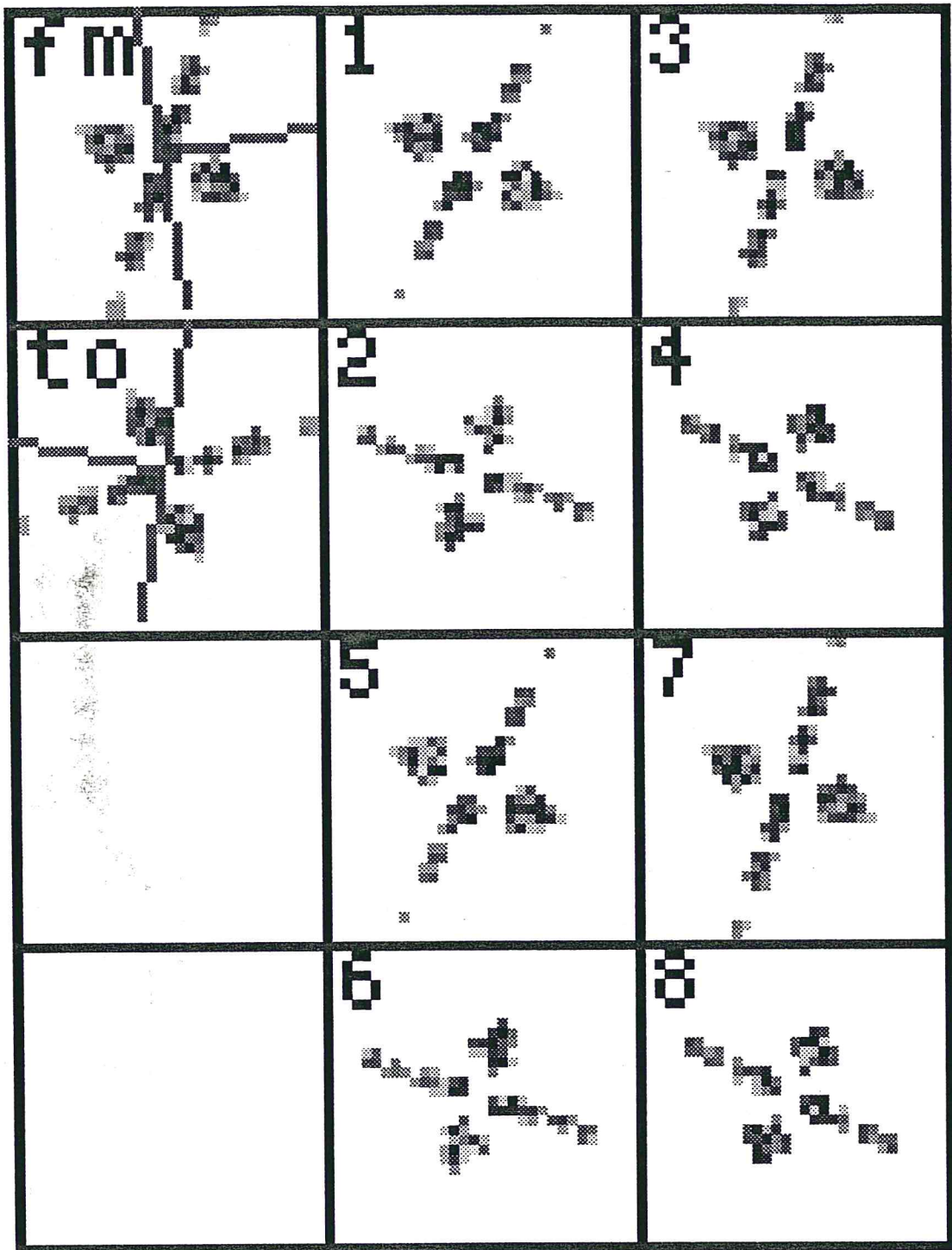


Figure 11: *From-block, to-block* and eight transformed blocks

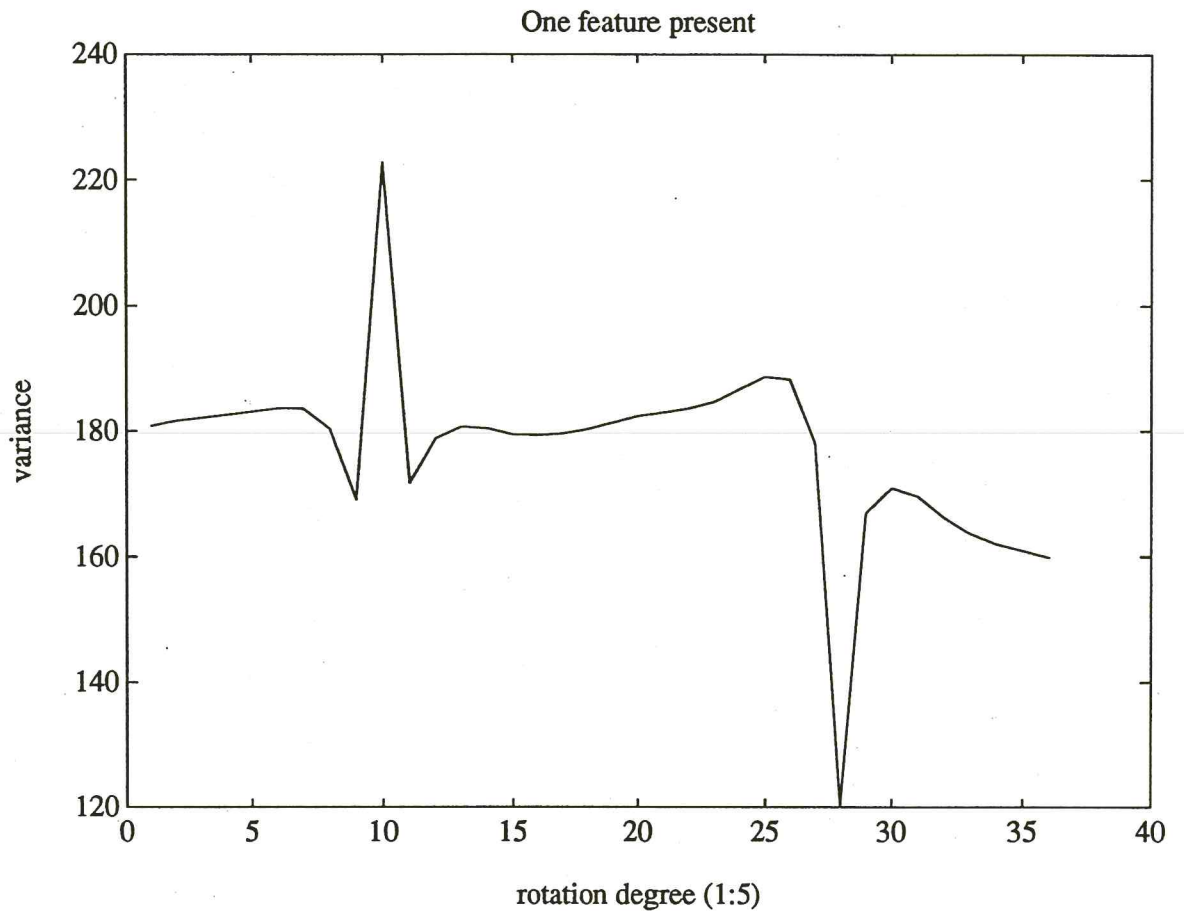


Figure 12: Plot of variance vs. rotation degree (one feature case)

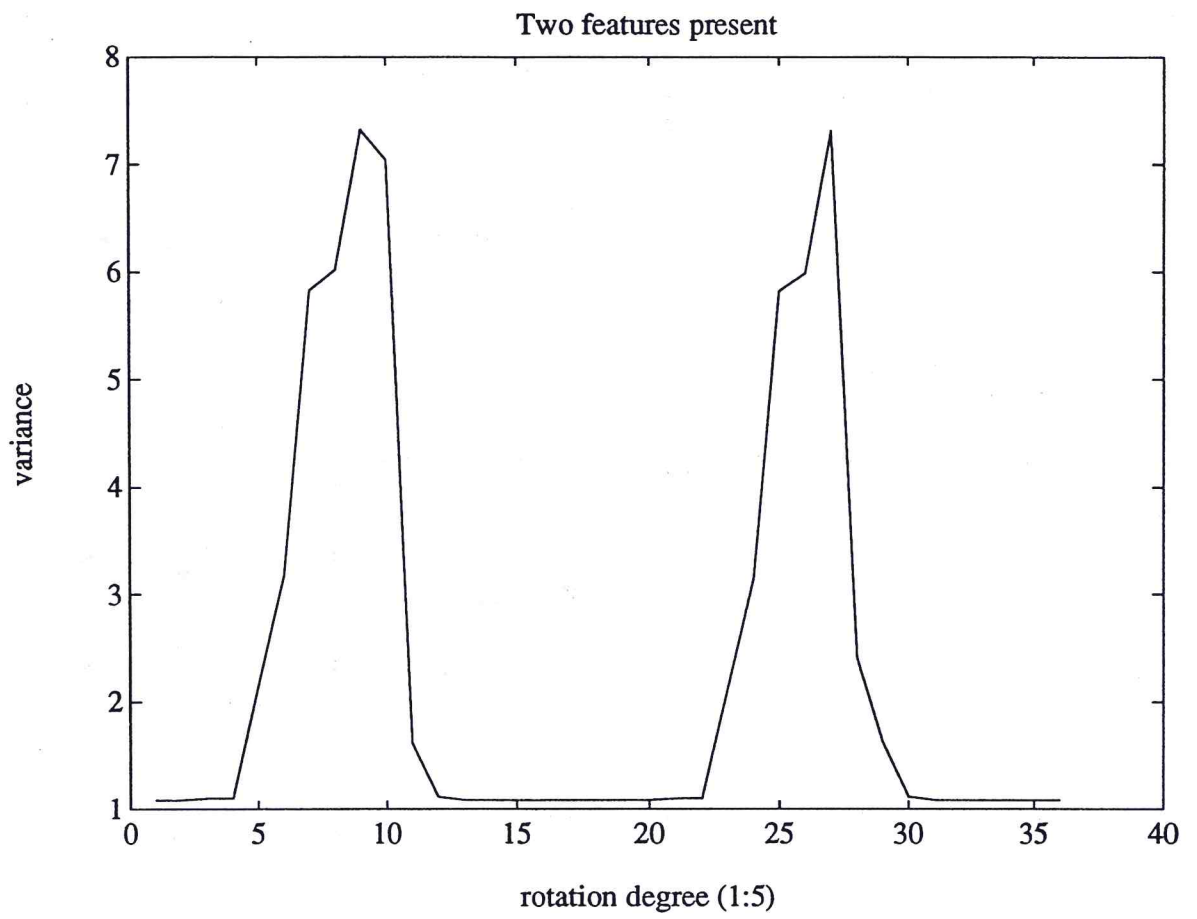


Figure 13: Plot of variance vs. rotation degree (two features case)

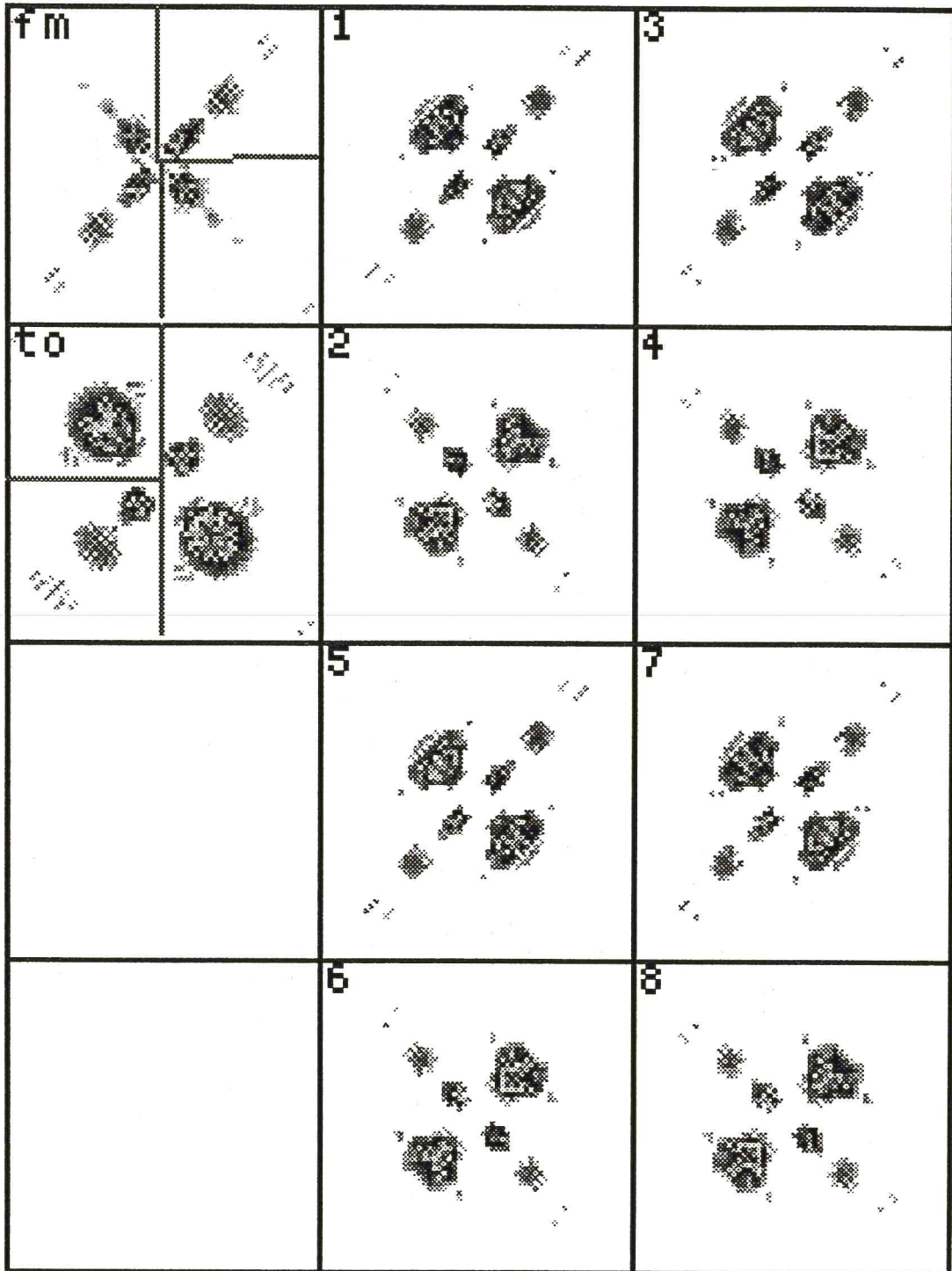


Figure 14: Algorithm failed when the MFT block of size 64×64

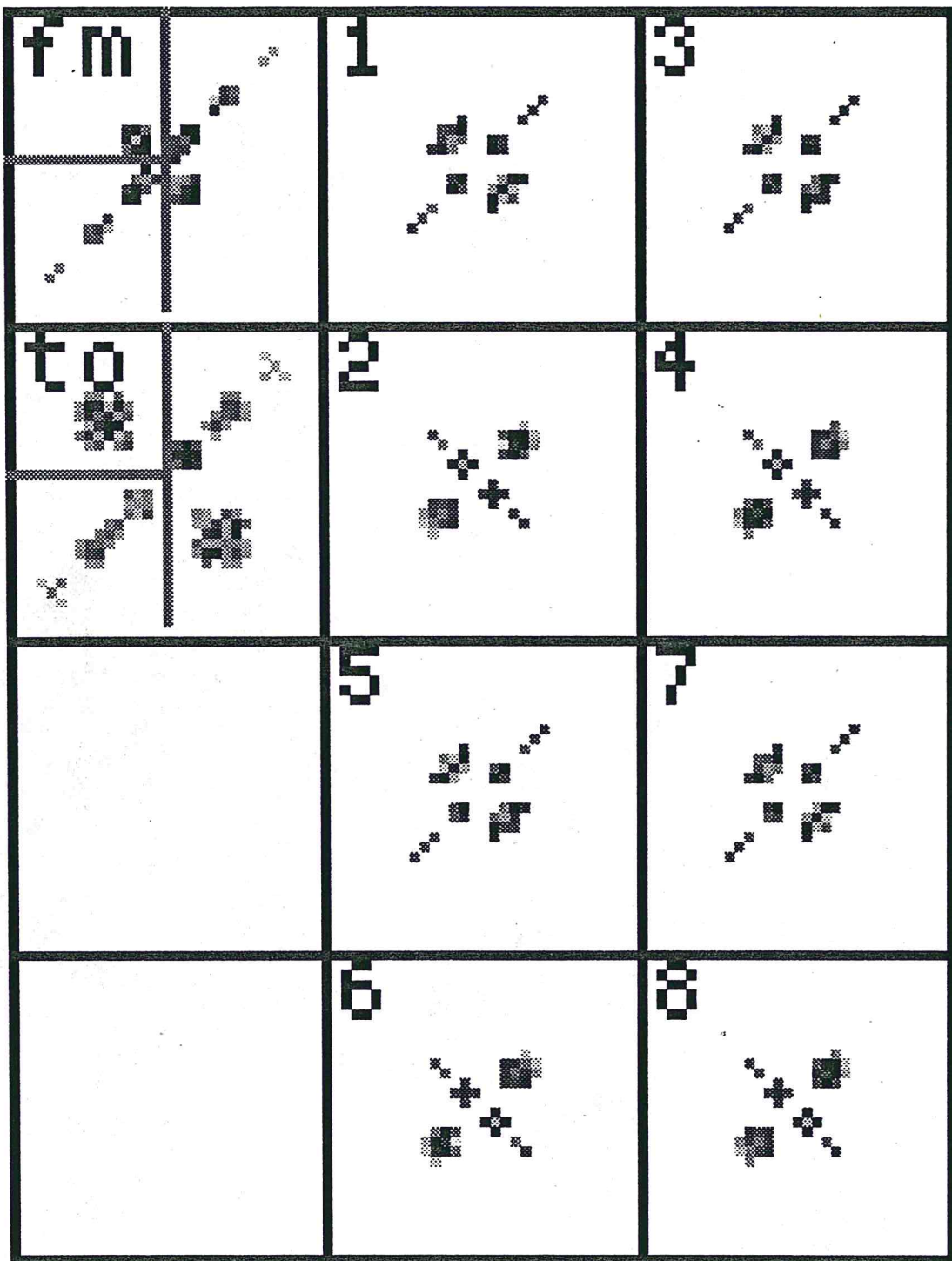


Figure 15: Smaller MFT block size (32×32) solves the mistaken selection



Figure 16: FM pattern synthesis at MFT level 6

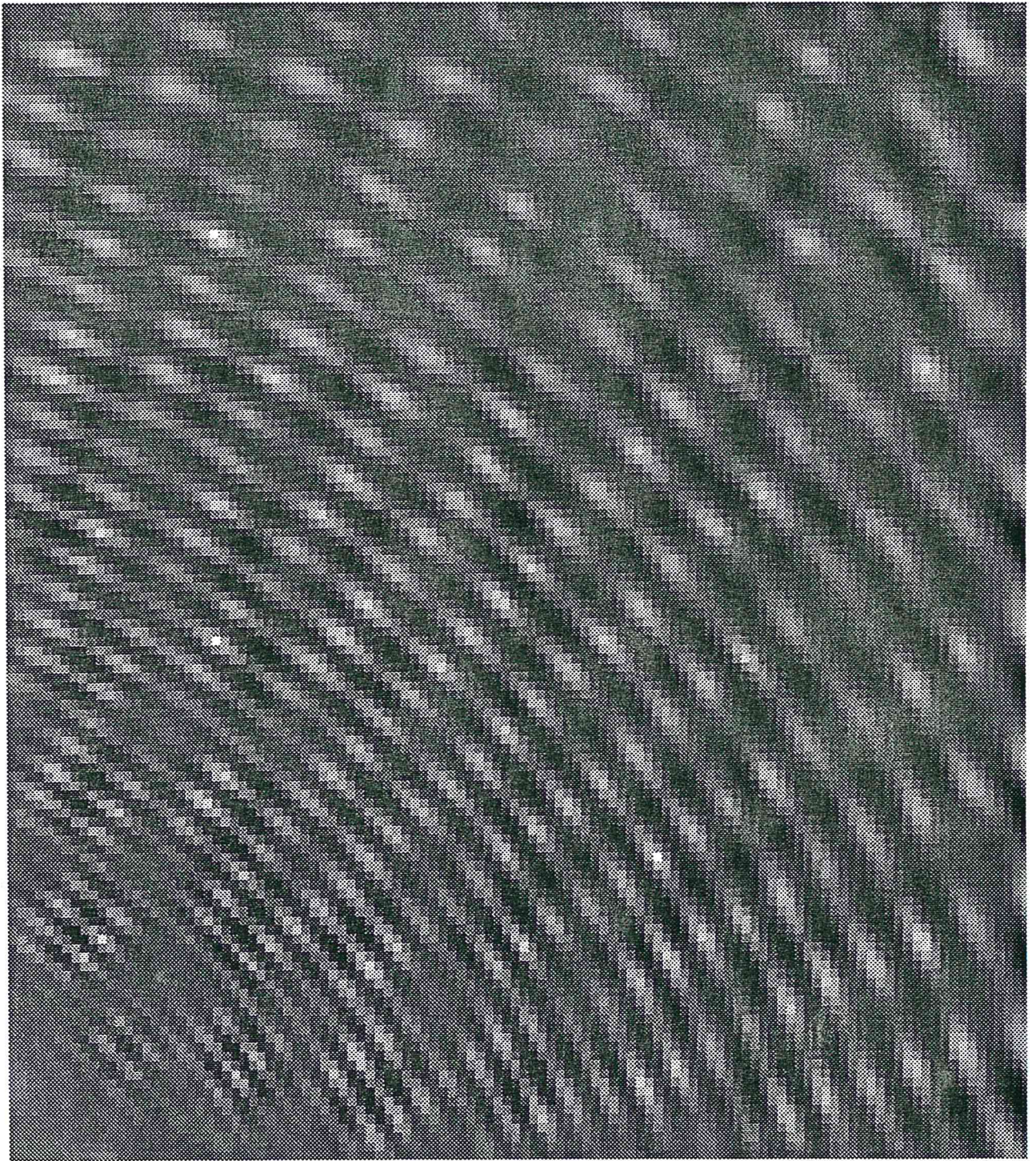


Figure 17: FM pattern synthesis at MFT level 5

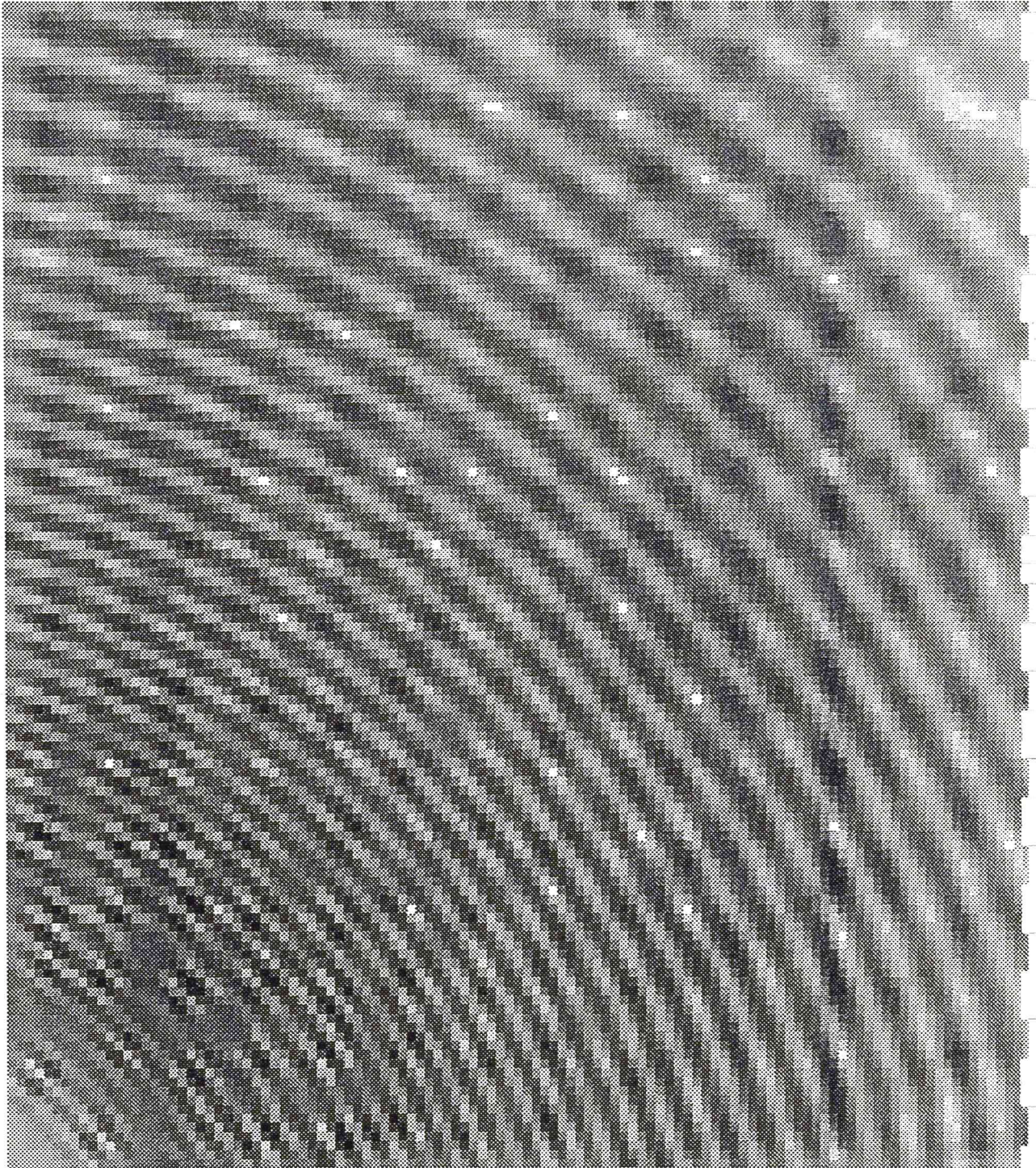


Figure 18: FM pattern synthesis at MFT level 4

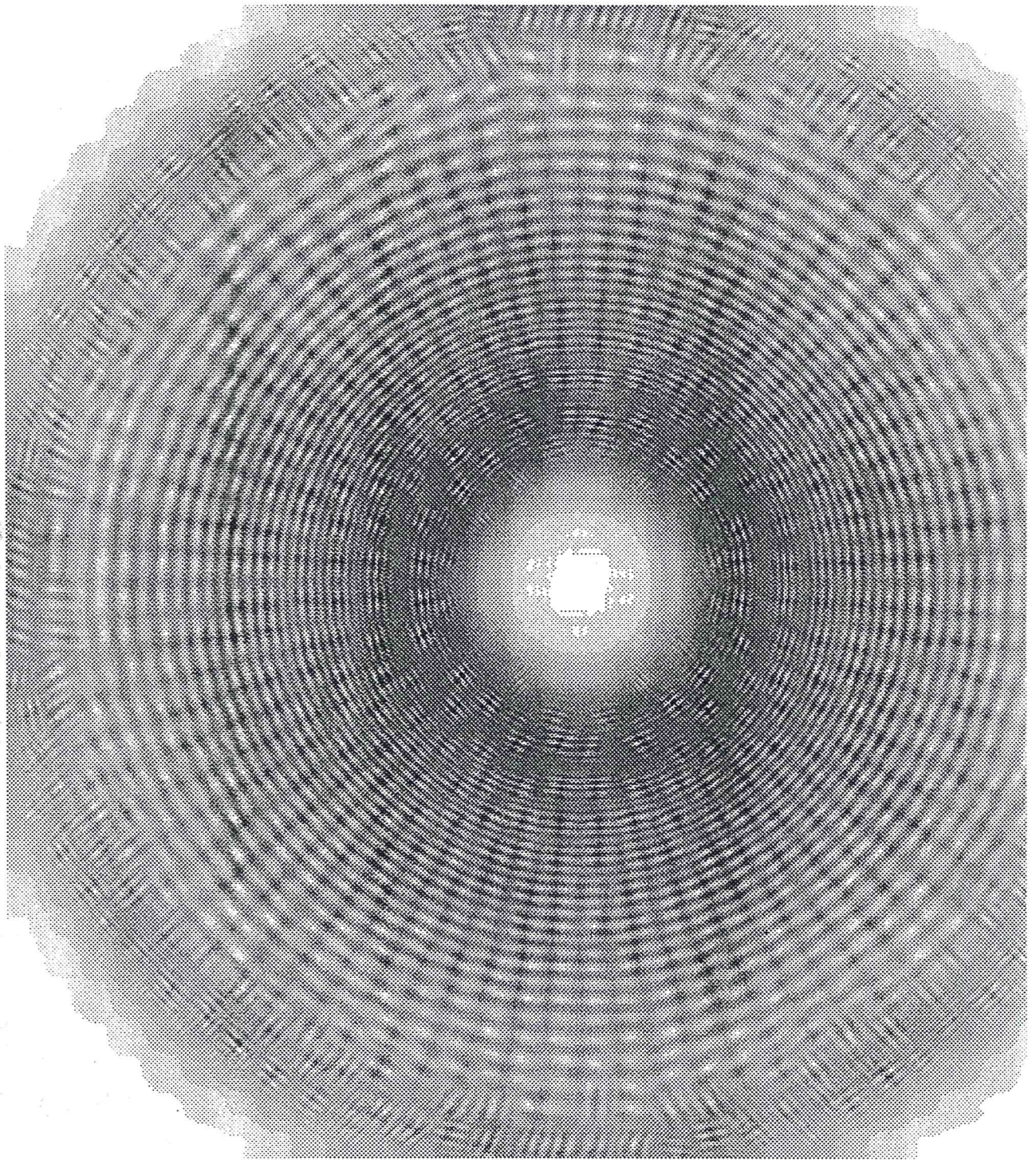


Figure 19: Entire FM pattern synthesis at MFT level 5

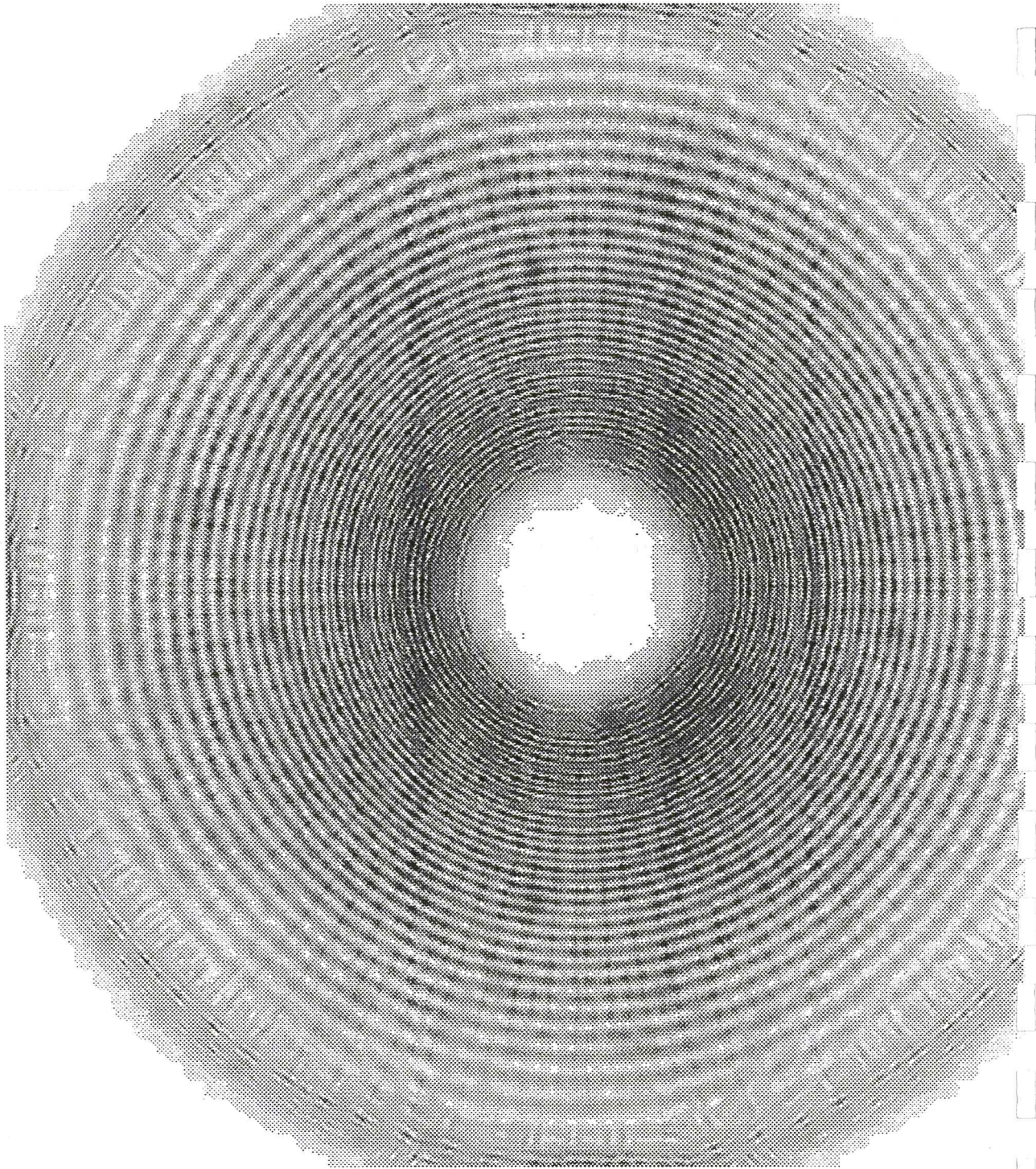


Figure 20: Entire FM pattern synthesis at MFT level 4

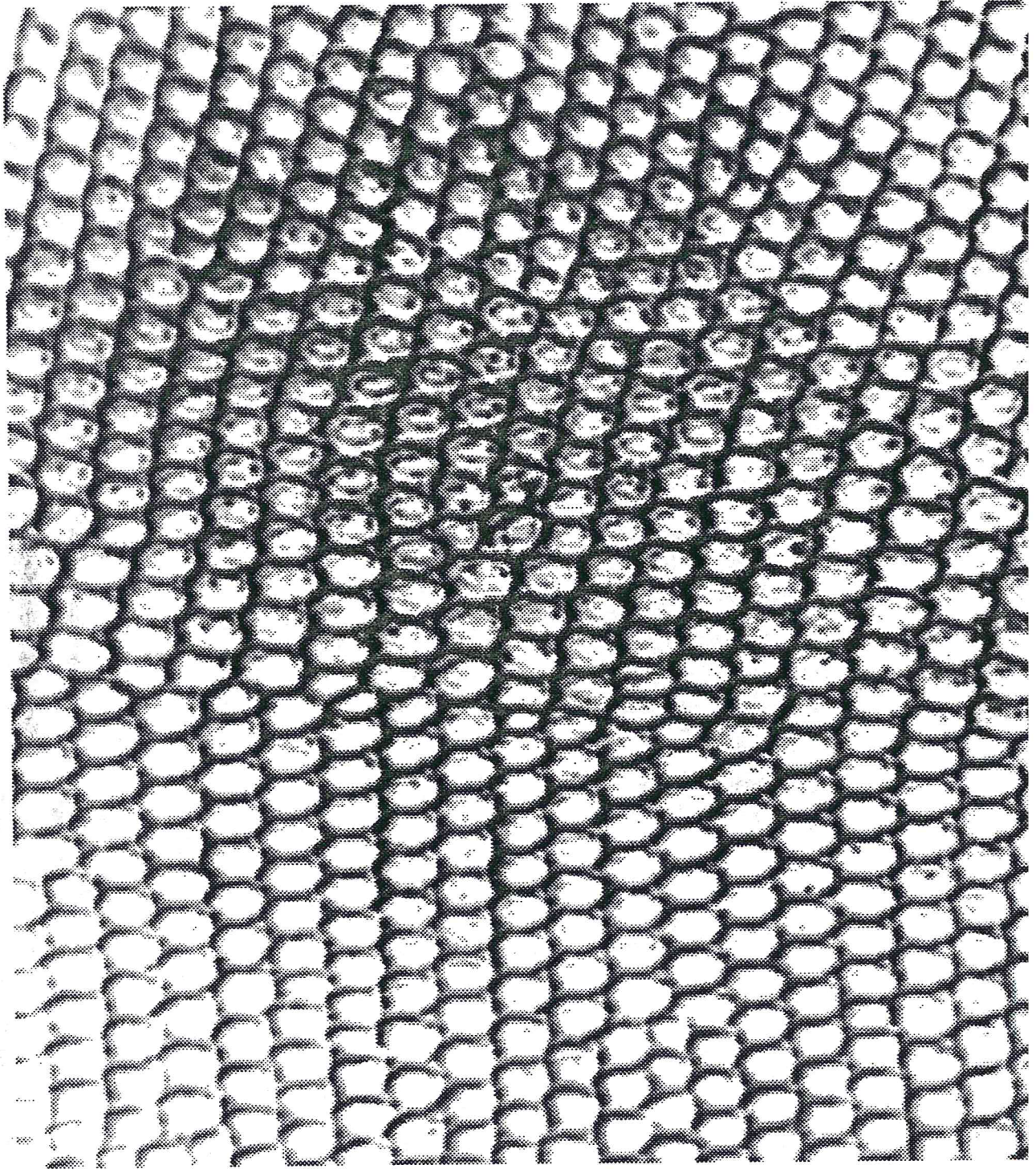


Figure 21: Original reptile pattern

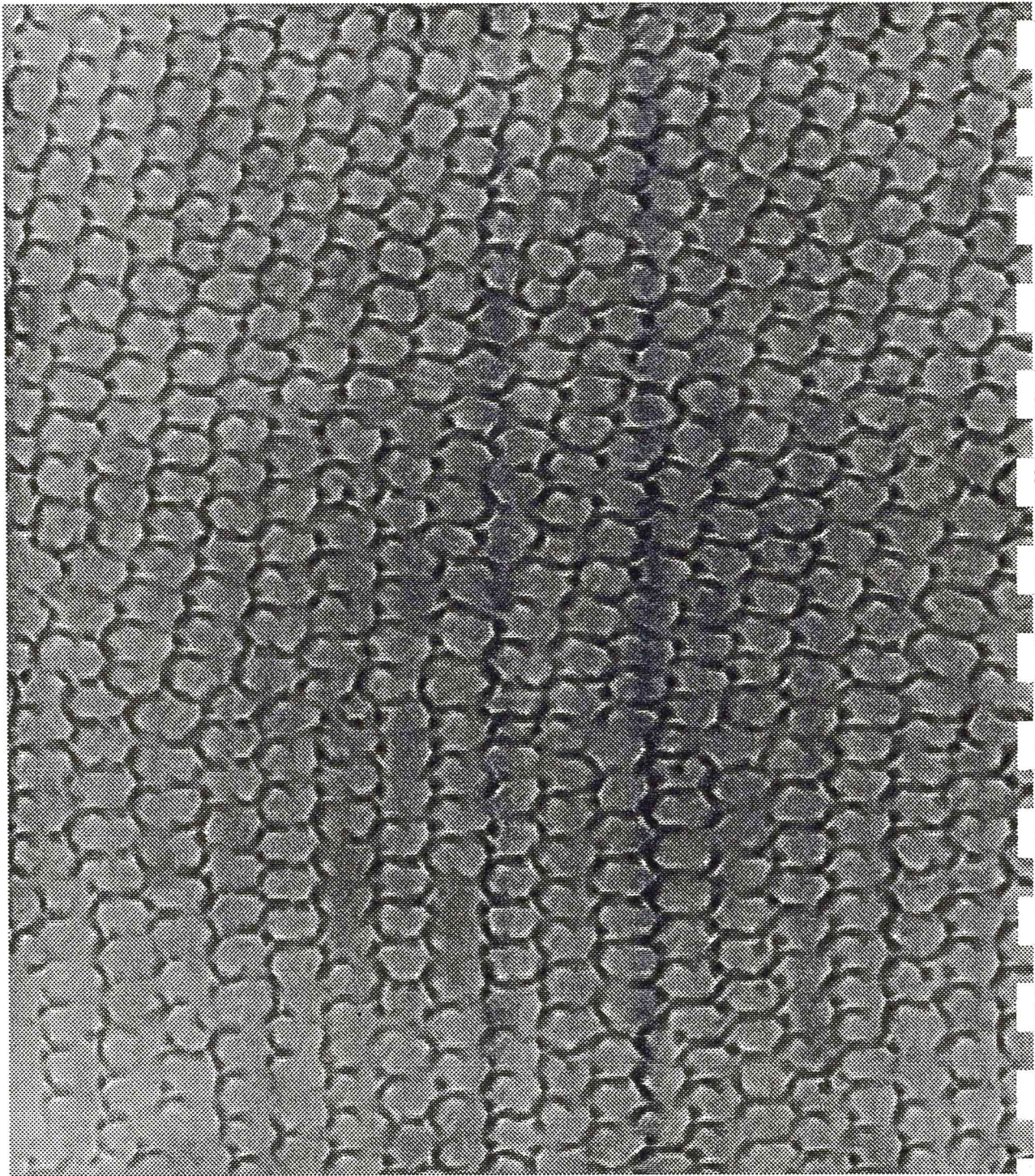


Figure 22: Reptile pattern synthesis at MFT level 5



a.Reptile synthesized at MFT level 3.



b.Reptile synthesized at MFT level 4.

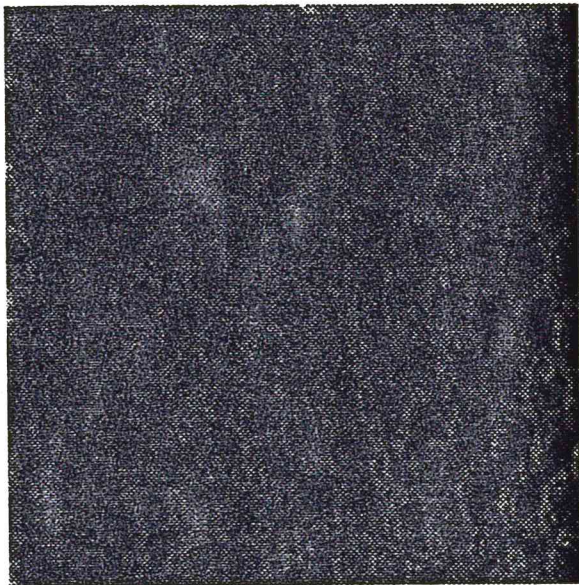


c.Reptile synthesized at MFT level 5.



d.Reptile synthesized at MFT level 6.

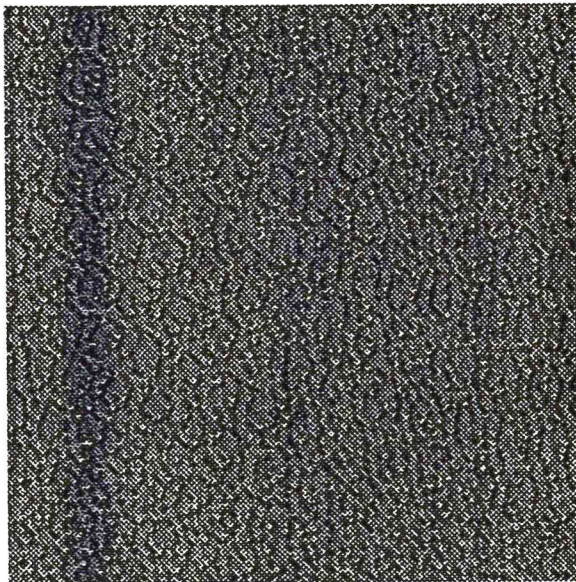
Figure 23: Reptile pattern synthesis at MFT level 3,4,5 and 6



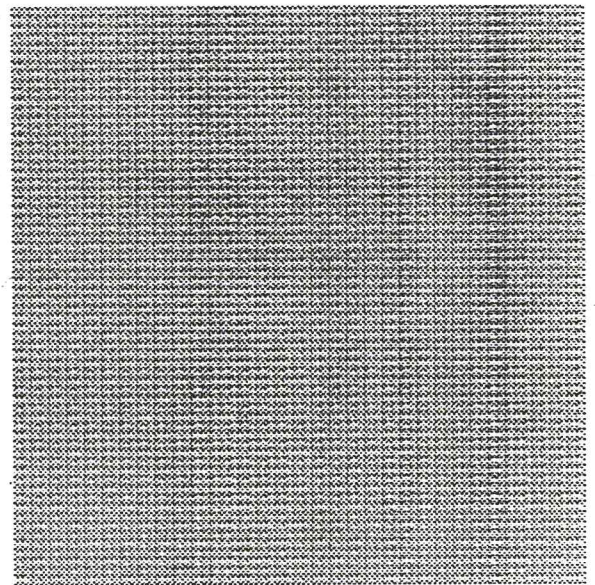
a.Reptile synthesized at MFT level 3.



b.No energy normalization.



c.No energy normalization and transform.



d.No energy normalization, transform and shift.

Figure 24: The significance of different functions